

Supplementary information

Mechanism of zinc oxide nanoparticle entry into wheat seedling leaves†

Jiahui Zhu,^{ab} Jinfeng Li,^a Yu Shen,^{a,c} Shiqi Liu,^a Nengde Zeng,^a Xinhua Zhan,^{*a} Jason C. White,^c Jorge Gardea-Torresdey,^d and Baoshan Xing^{*b}

* Corresponding authors: Dr. Xinhua Zhan

Phone: +86-25-84395210

E-mail: xhzhan@njau.edu.cn

* Corresponding author: Dr. Baoshan Xing

Tel.: +1 (413) 545-5212

E-mail: bx@umass.edu

^a College of Resources and Environmental Sciences, Nanjing Agricultural University, Nanjing, Jiangsu Province, 210095, People's Republic of China

^b Stockbridge School of Agriculture, University of Massachusetts, Amherst, Massachusetts 01003, United States

^c Department of Analytical Chemistry, The Connecticut Agricultural Experiment Station, New Haven, CT, 06504, United States

^d Department of Chemistry and Biochemistry, University of Texas at El Paso, 500 West University Ave., El Paso, TX 79968, United States

Supplementary materials and methods

Nanoparticle size

50 μL 100 $\mu\text{mol L}^{-1}$ zinc oxide nanoparticles (ZnO NPs) suspension were drop-deposited onto Cu grid and dried.¹ The size of ZnO NPs was detected by a transmission electron microscope (Hitachi, H-3000 N, Japan, 80.0 kV) and a scanning electron microscope (Hitachi SU8010, Japan, 6.0 kV).

Releasing of FITC from FITC-ZnO NPs

100 $\mu\text{mol L}^{-1}$ FITC-ZnO NPs were dispersed in the solutions with different pH values (5.8 and 7.0) by ultrasonic treatment (25 °C, 100 W, 40 kHz) with stirring for 1 h to achieve a stable dispersion. Samples were collected at five time points (2, 4, 8, 16 and 24 h) after the dispersion; the supernatants and precipitates were collected after being centrifuged at 8000 g (4 °C) for 15 min. Images of all samples (supernatants and precipitates) were taken under a fluorescence microscope (Nikon 80i, Japan) attached with a CCD (charge coupled device) camera. FITC was detected by blue filter (excitation) and green filter (emission) in the fluorescence microscopic observation.

Wheat leaf tissues confocal laser scanning microscope images in control and FITC only groups

100 $\mu\text{mol L}^{-1}$ FITC/ABA solution and deionized water were sprayed on the wheat seedling leaves (40 μL per exposed leaf). All solutions/suspensions were sprayed with small hand-held- spray bottles. Sampling was performed by using a cork borer at

different time points (2, 4, 8, 16 and 24 h) after foliar application. Then, all tissues were mounted on microscope slides after being rinsed with deionized water and dried. An observation gel well (5 mL neutral resins for every 1 mL xylene, 1 mm thin) was made for mounting the wheat leaf discs. Leaf tissue was placed in the center of the observation gel. Afterward, a coverslip was placed on the top of leaf tissue carefully to seal it into the well, ensuring that no bubbles remain trapped underneath. All the prepared sample slides were evaluated with a white light laser confocal microscope (TCS SP8, Germany). A 40 × objective was used in the observation. Excitation/emission wavelengths for FITC and chloroplast were 488/519 nm and 488/650 nm in the laser confocal microscopic observation, respectively. Five sample slides from each treatment were used for observation.

SEM-EDS images of ZnO NPs on wheat leaf surfaces

Fresh wheat seedling leaf tissues were divided into two groups. Two groups were treated with 1 mmol L⁻¹ and 100 μmol L⁻¹ ZnO NPs (40 μL per exposed leaf) for 24 h, respectively. After that, half of the wheat seedling leaves were washed immediately by deionized water with a wash bottle in each group. Scanning electron microscopy–energy dispersive X-ray spectroscopy (SEM-EDS and elemental mapping, Hitachi SU8010, Japan) was used to detect and map the Zn on wheat leaf surface.

Yield of ZnO NPs after centrifugation

100 $\mu\text{mol L}^{-1}$ ZnO NPs (*i.e.* 8.1 mg L^{-1}) were suspended in the solutions with different pH values (5.8, 7.0 and 7.5). The solution of ZnO NPs was dispersed with ultrasonicator (25 °C, 100 W, 40 kHz) with stirring for 1 h before use. Plastic centrifuge tube weights were recorded, and then the sampled ZnO NPs suspensions were transferred into the tubes. After being centrifuged at 8000 g for 15 min, the supernatants were removed and the tubes with precipitates of ZnO NPs were dried in a drying oven. Afterward, the weights of tubes with precipitates were measured. Six replicates were conducted for each treatment. Yield (%) = (weight of tube with precipitate – tube weight)/initial weight \times 100.

Supplementary Tables

Table S1 Characterizations of zinc oxide nanoparticles (ZnO NPs) suspension, fluorescein isothiocyanate (FITC)-ZnO NPs suspension and ZnSO₄ solution at 100 $\mu\text{mol L}^{-1}$. Results are expressed as means \pm standard deviation of triplicates. Different letters for each column indicate significant difference at $P < 0.05$ according to *Duncan's* test.

Treatment	Average hydrodynamic diameter (nm)	Zeta potential (mV)	pH	Conductivity ($\mu\text{s cm}^{-1}$)
ZnO NPs	341.20 \pm 45.41a	-16.3 \pm 4.94a	7.56 \pm 0.32a	1.70 \pm 0.11b
FITC-ZnO NPs	363.90 \pm 56.24a	-19.4 \pm 3.30a	7.50 \pm 0.29a	1.67 \pm 0.16b
ZnSO ₄	—	—	6.64 \pm 0.25b	50.97 \pm 4.01a

Table S2 Yield of ZnO NPs after centrifugation at different pH values. Results are expressed as means \pm standard deviation of sextuplicates. Different letters indicate significant difference at $P<0.05$ according to *Duncan`s* test.

Treatment	Yield (%)
pH 5.8	74.69 \pm 2.56b
pH 7.0	90.53 \pm 2.43a
pH 7.5	91.98 \pm 3.10a

Supplementary figures

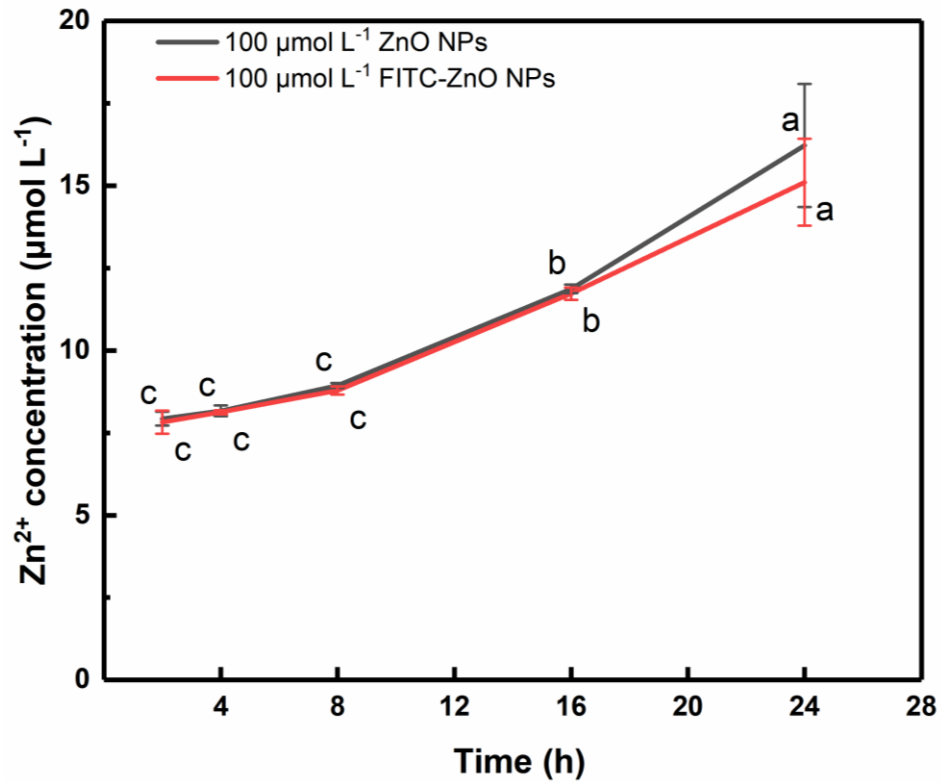
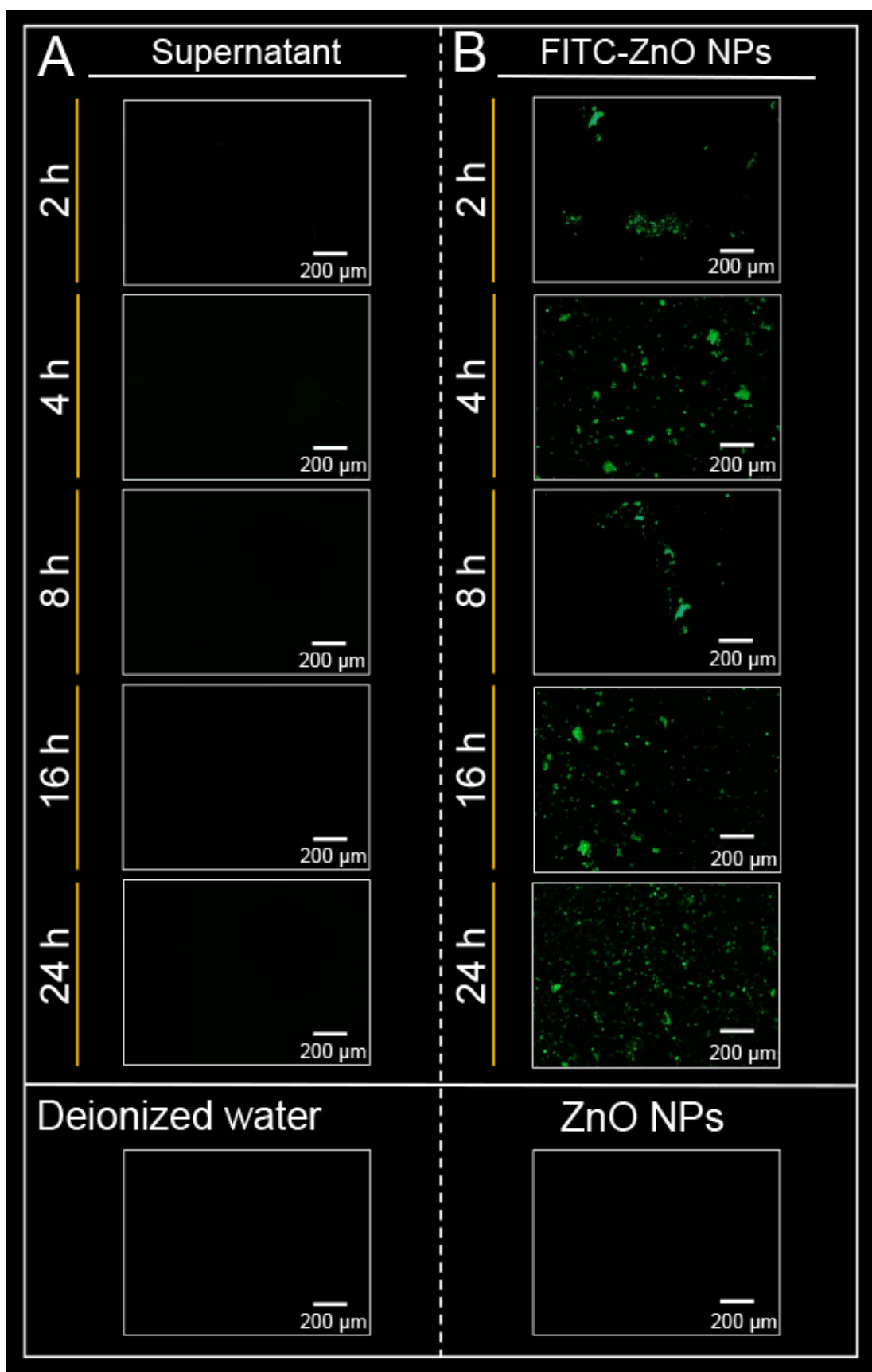


Fig. S1 Time-dependent dissolution of 100 µmol L⁻¹ zinc oxide nanoparticles and fluorescein isothiocyanate (FITC)-zinc oxide nanoparticles (FITC-ZnO NPs) in deionized water. Data points represent mean and standard deviation values of triplicates. Different letters indicate significant difference at $P < 0.05$ according to *Duncan's* test.



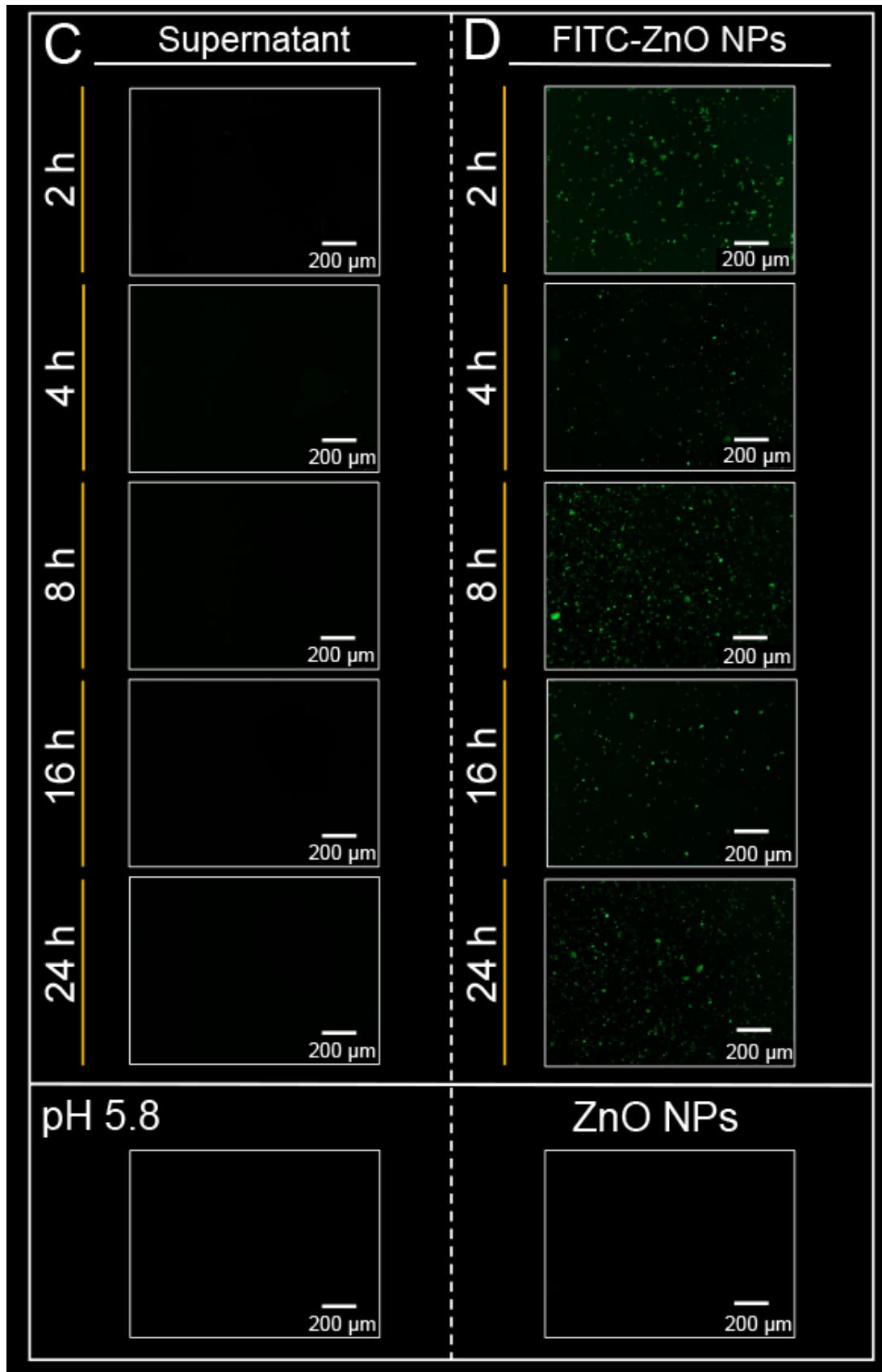


Fig. S2 Fluorescence microscope images of fluorescein isothiocyanate released in the supernatant (A, C) and remained on FITC-ZnO NPs (B, D) from fluorescein isothiocyanate-zinc oxide nanoparticles at different time and pH values.

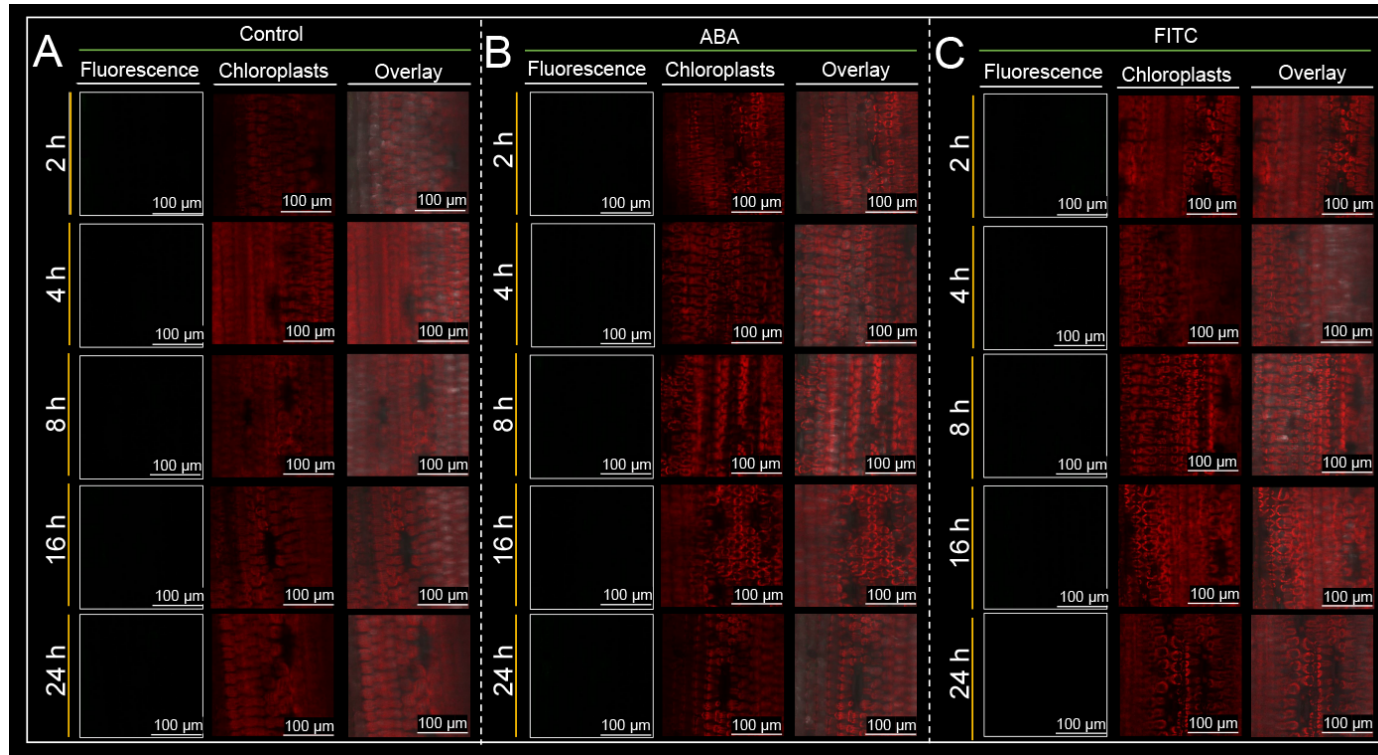


Fig. S3 Confocal laser scanning microscopy images of wheat leaves treated with deionized water (A), 100 $\mu\text{mol L}^{-1}$ abscisic acid (B) and 100 $\mu\text{mol L}^{-1}$ fluorescein isothiocyanate (C) at different time.

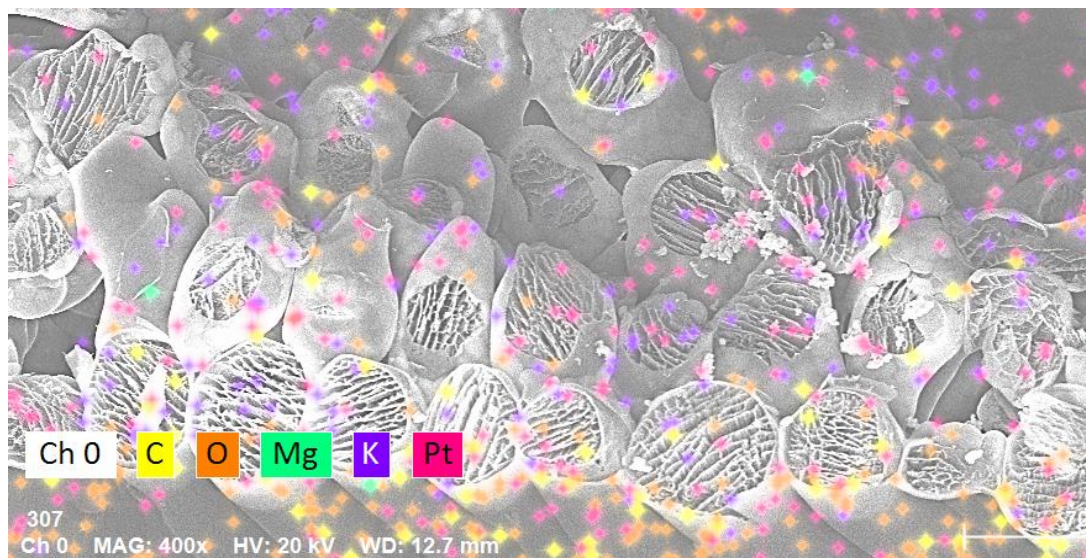


Fig. S4 Scanning electron microscope elemental mapping of wheat leaf sections without zinc oxide nanoparticles and ZnSO_4 .

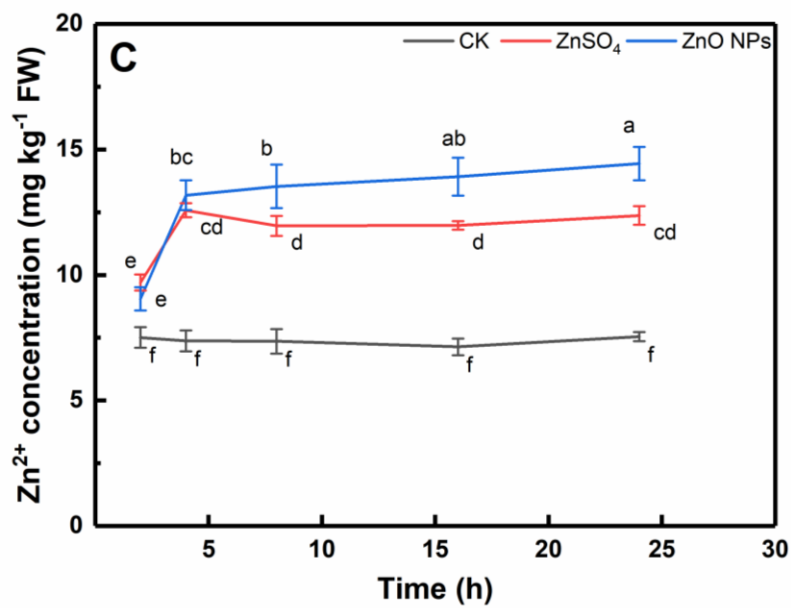
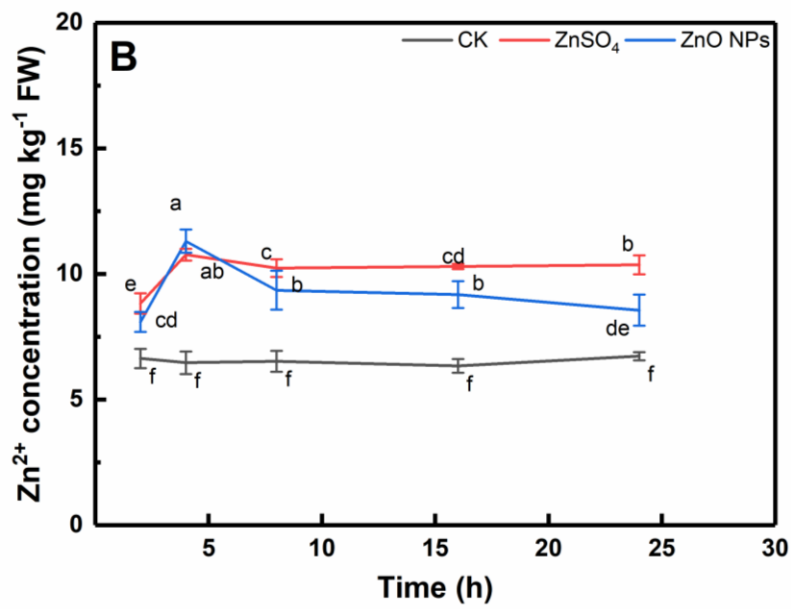
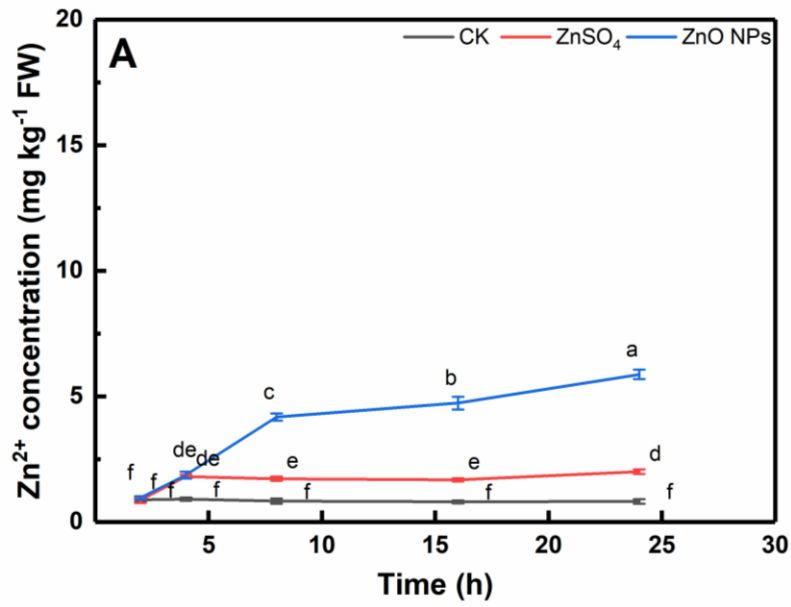


Fig. S5 Zn^{2+} concentrations in wheat leaf apoplast (A), cytoplasm (B) and wheat leaves (C) at different time points. ZnSO_4 , N and CK present wheat leaves treated with $100 \mu\text{mol L}^{-1}$ ZnSO_4 , $100 \mu\text{mol L}^{-1}$ zinc oxide nanoparticles (ZnO NPs) and deionized water, respectively. FW, fresh weight. Data points represent mean and standard deviation values of triplicates. Different letters in the same figure indicate significant difference at $P < 0.05$ according to *Duncan's* test.

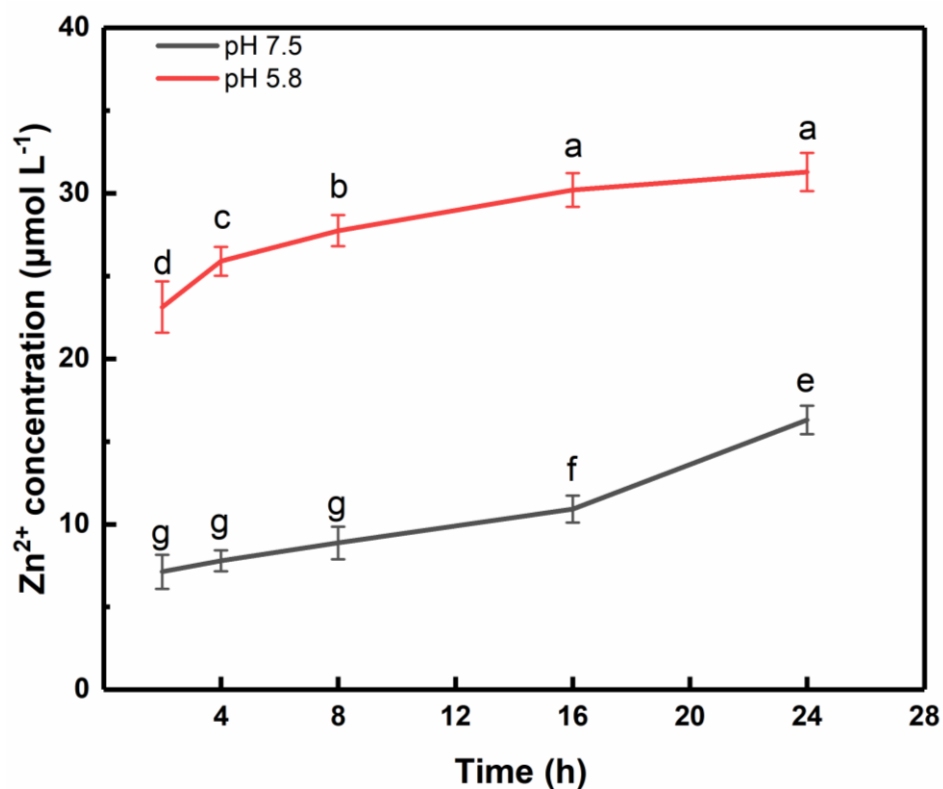


Fig. S6 Time-dependent dissolution of 100 $\mu\text{mol L}^{-1}$ zinc oxide nanoparticles at different pH values. Data points represent mean and standard deviation values of triplicates. Different letters indicate significant difference at $P < 0.05$ according to *Duncan's* test.

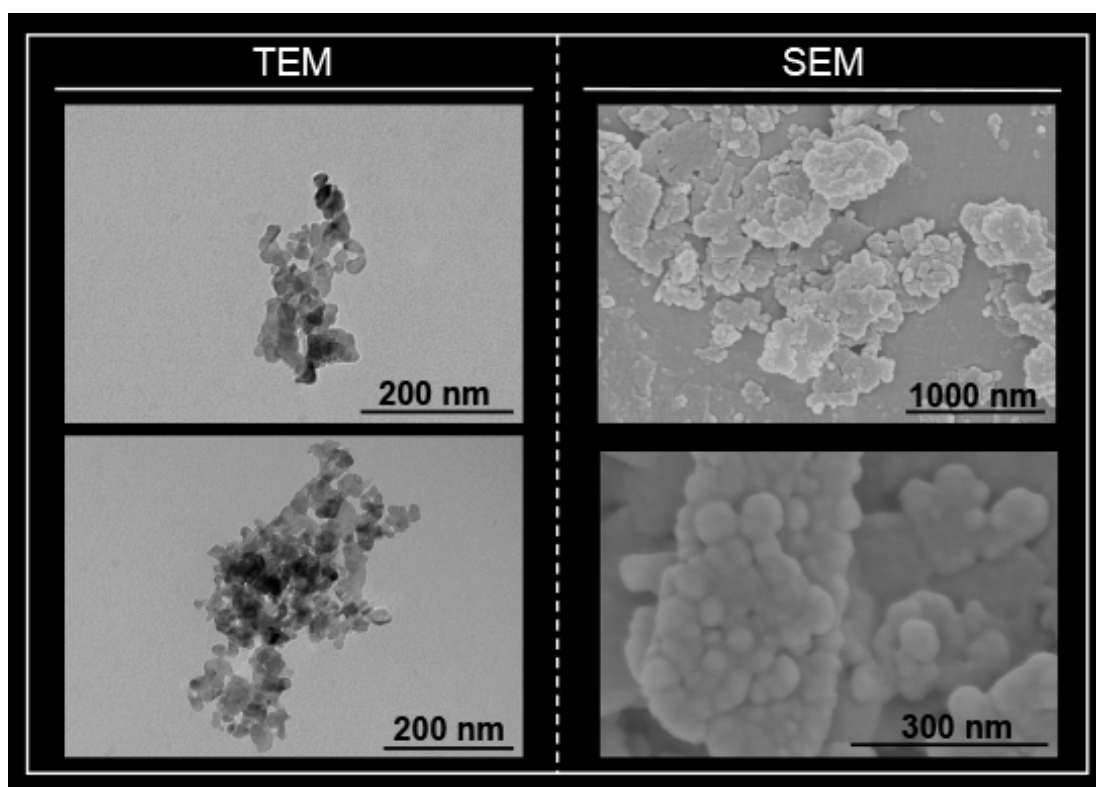
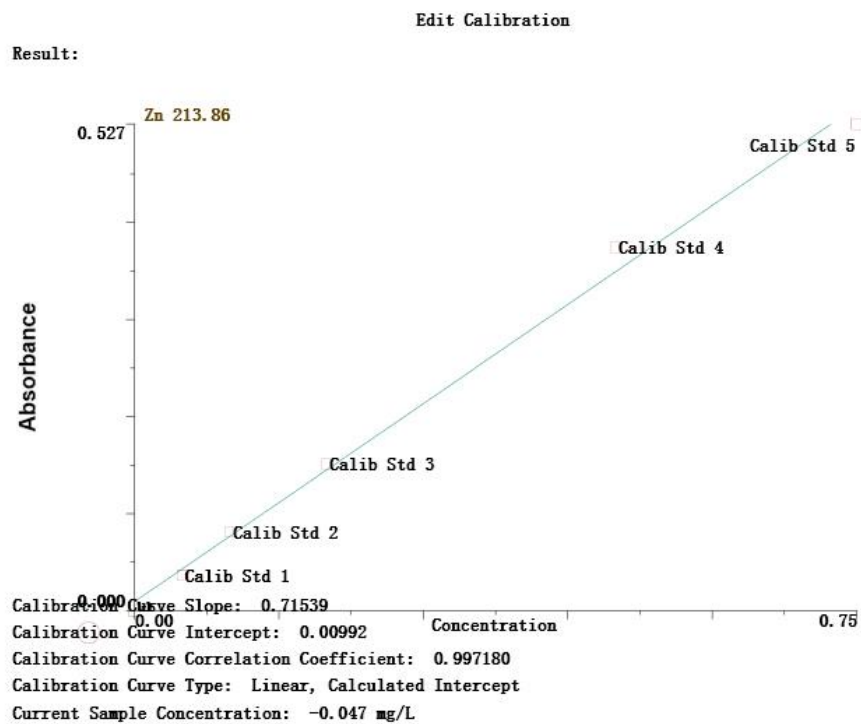


Fig. S7 Scanning electron microscope (SEM) and transmission electron microscope (TEM) images of zinc oxide nanoparticles.



Std #	Standard ID	Entered Conc.	Calculated Conc.	Action
Blank	kb	0	-0.014	Include
1	Calib Std 1	0.05	0.040	Include
2	Calib Std 2	0.10	0.106	Include
3	Calib Std 3	0.20	0.208	Include
4	Calib Std 4	0.50	0.537	Include
5	Calib Std 5	0.75	0.723	Include

Fig. S8 The working curve of flame atomic absorption spectrophotometer.

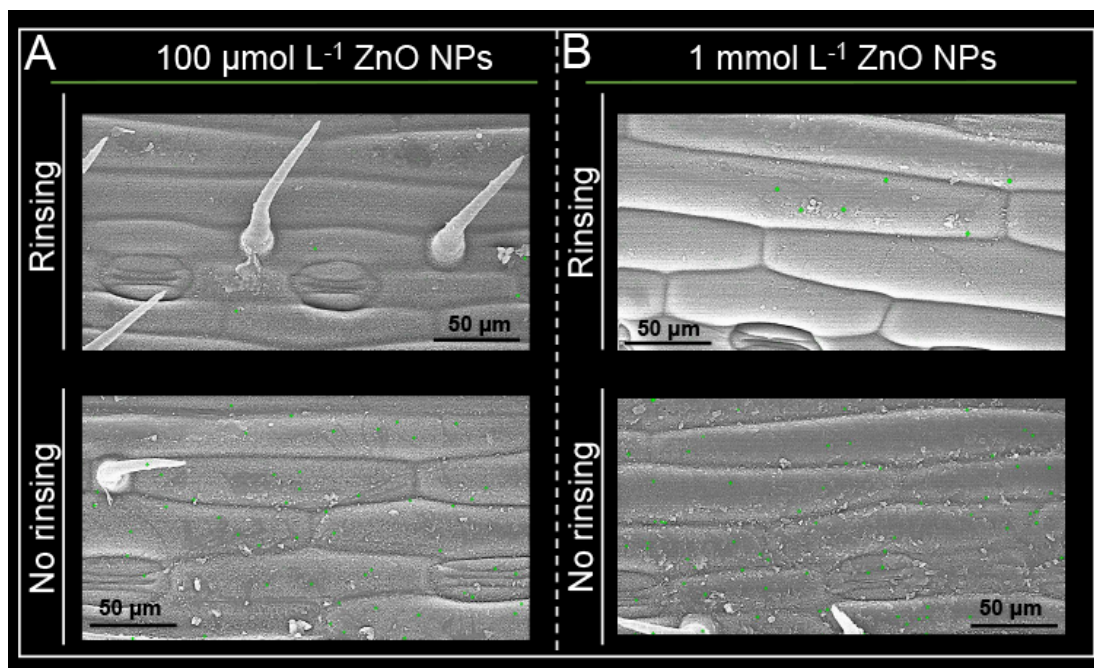


Fig. S9 Scanning electron microscope-energy dispersive X-ray spectroscopy images of $100 \mu\text{mol L}^{-1}$ (A) and 1 mmol L^{-1} (B) zinc oxide nanoparticles (ZnO NPs) on wheat leaf surface.

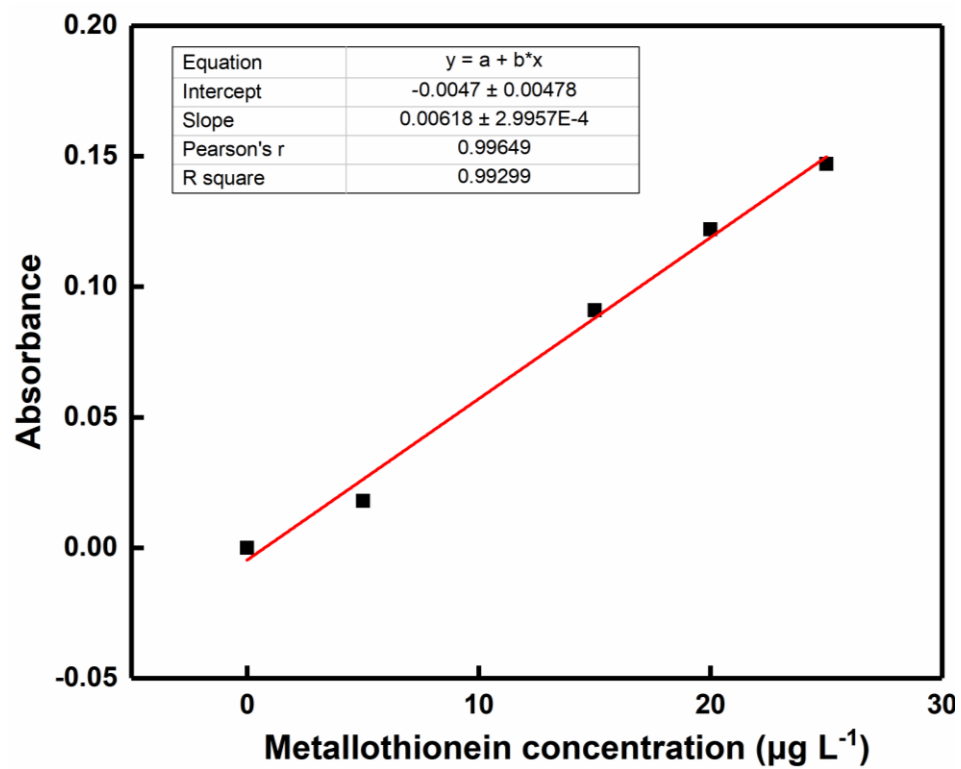


Fig. S10 The standard curve for metallothionein concentration calculation.

References

- 1 A. Avellan, J. Yun, Y. Zhang, E. Spielman-Sun, J. M. Unrine, J. Thieme, J. Li, E. Lombi, G. Bland and G. V. Lowry, *ACS Nano*, 2019, **13**, 5291-5305.